Inorganic Chemistry

Article

pubs.acs.org/IC

Ligand-Localized Triplet-State Photophysics in a Platinum(II) Terpyridyl Perylenediimideacetylide

Valentina Prusakova, Catherine E. McCusker, and Felix N. Castellano*

Department of Chemistry and Center for Photochemical Sciences, Bowling Green State University, Bowling Green, Ohio 43403, United States

Supporting Information

ABSTRACT: The synthesis, electrochemistry, and photophysical behavior of a Pt(II) terpyridyl perylenediimide (PDI) acetylide (**1**) charge-transfer complex is reported. The title compound exhibits strong ($\varepsilon \approx 5 \times 10^4$ $M^{-1}cm^{-1}$) low-energy PDI acetylide-based $\pi-\pi^*$ absorption bands in the visible range extending to 600 nm, producing highly quenched singlet fluorescence ($\Phi = 0.014 \pm 0.001$, $\tau = 109$ ps) with respect to a nonmetalated PDI model chromophore. Nanosecond transient absorption spectroscopy revealed the presence of a long excited-state lifetime (372 ns in 2-methyltetrahydrofuran) with transient features consistent with the PDI−acetylide triplet state, ascertained by direct comparison to a model Pt(II) PDI−acetylide complex lacking low-energy charge-transfer transitions. For the first time, time-resolved step−scan FT-IR spectroscopy was used to characterize the triplet excited state of the PDI−acetylide sensitized in the title compound and its associated model complex. The observed red shifts (~30−50 cm^{-1}) in the C═O and C≡C vibrations of the two Pt(II) complexes in the long-lived excited state are consistent with formation of the ^{3}PDI acetylide state and found to be in excellent agreement with the expected change in the relevant DFT-calculated IR frequencies in the nonmetalated PDI model chromophore (ground singlet state and lowest triplet excited state). Formation of the PDI triplet excited state in the title chromophore was also supported by sensitization of the singlet oxygen photoluminescence centered at ~1275 nm in air-saturated acetonitrile solution, $\Phi(^1O_2) = 0.52$. In terms of light emission, only residual PDI-based red fluorescence could be detected and no corresponding PDI-based phosphorescence was observed in the visible or NIR region at 298 or 77 K in the Pt(II) terpyridyl perylenediimideacetylide.

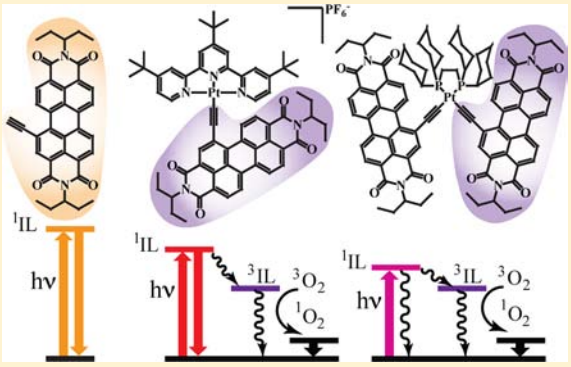

INTRODUCTION

The photophysical properties of Pt(II) terpyridyl acetylide complexes have been intensively investigated for approximately a decade.[1−72] The square planar geometry of these complexes provides the opportunity for a variety of intermolecular interactions in their ground and excited states.[1−26] Notably, the photophysical properties of these Pt(II) complexes can be easily tuned through incorporation of substituents in the 4′ position of the terpyridyl and/or variation in the alkyl/arylacetylide ligands.[21−25,27−34,73−75] The terpyridyl ligand introduces additional rigidity into the molecule, which significantly reduces nonradiative decay due to the D_{4h} to D_{2d} distortion in the excited state with respect to the analogous bipyridyl complexes.[22,28,73,76] However, the significant size of the Pt(II) center leads to a geometry exhibiting a Pt−N central bond shortened with respect to the two peripheral ligation points and N−Pt−N bite angles of 79.1° and 80.5°.[76] As a result the ligand field is reduced, thereby lowering the respective d−d states in energy and making them a viable pathway for excited-state deactivation.[22,28,73,76] However, incorporation of a strong-field acetylide ligand shifts the deactivating ligand field states higher in energy, rendering these compounds emissive in room-temperature solutions. This trivial manipulation of photophysical properties renders such molecules promising chromophores for optical power limiting,[24,29,31,32,52] singlet oxygen photosensitization,[39,40] photocatalytic hydrogen production,[24,41−45,71] luminescence sensing,[7,24,25,34,46−50,72] electrogenerated chemiluminescence,[66] dye-sensitized solar cells,[67] biolabeling,[1,12,24,35] photoinduced charge separation (artificial photosynthesis),[38] and DNA metallointercalation.[56]

Growing interest in the development of photovolatics and solar fuels catalysis requiring visible-absorbing chromophores with high oscillator strength has led to perylenediimides (PDI) being incorporated into transition metal complexes in a variety of formats.[78−84] PDIs are stable, low-cost organic dyes with high molar absorptivities, high fluorescence quantum yields, and tunable spectroscopic properties that have resulted in their widespread investigation as chromophores in a myriad of electron- and energy-transfer cascades as well as applications in molecular electronics and photovoltaics.[85−90] The performance of photovoltaic devices and light-emitting electrochemical cells may potentially be improved by accessing the long-lived PDI

Received: June 1, 2012
Published: July 18, 2012

   dx.doi.org/10.1021/ic301169t | Inorg. Chem. 2012, 51, 8589−8598

triplet excited states.[81,82,91,92] It has been previously demonstrated that the platinum−acetylide motif is particularly effective at promoting strong spin−orbit coupling from PDI subunit(s), thereby resulting in production of its lowest triplet excited state.[93−95] Relatedly, Rybtchinski and co-workers reported optoelectronically active supramolecular constructs derived from poly(ethylene oxide)-substituted PDIs fastened to a terpyridine ligand at its 4′ position using a phenyleneacetylene linker.[96,97] Incorporation of such organic building blocks into transition metal complexes of Pt(II), Pd(II), and Ag(I) resulted in a diversity of photonic superstructures. Furthermore, similar modules have been recently integrated into Pt(II)−peptide conjugates resulting in kinetically controlled self-assembled aggregates in aqueous media.[98] Notably, in these latter compositions, particularly those based on Pt(II), singlet state photophysics entirely dominates excited-state decay.

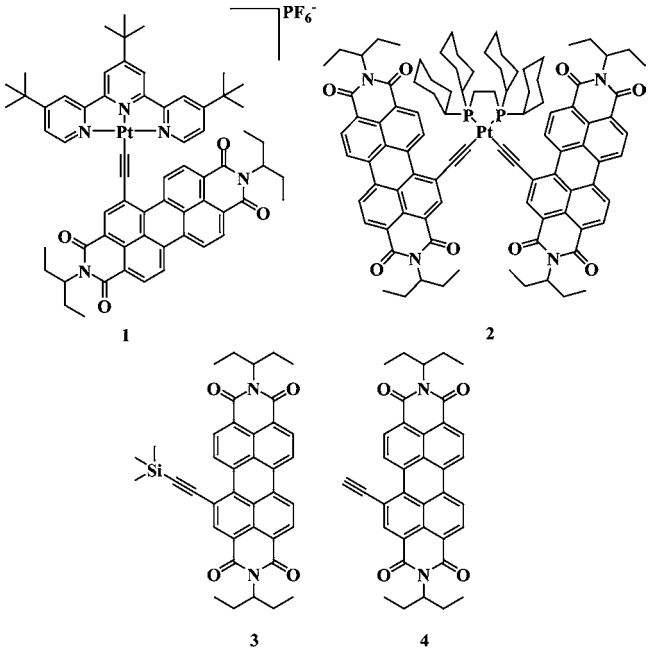

Interested in whether the PDI triplet state could indeed be accessed within the Pt(II) terpyridyl structural motif, we prepared a Pt(II) terpyridyl PDI−acetylide (**1**) where the PDI is covalently attached to the metal center through an acetylide linkage emanating from one of its bay positions. Complex **2** was chosen as a model "metal-perturbed" chromophore intended to mimic the photophysical and spectroscopic behavior of any IL states produced in **1** in the absence of any low-energy charge-transfer states. Compound **3** is the TMS-protected derivative of the terminal PDI−acetylene ligand **4**. An array of static and dynamic spectroscopic techniques including UV−vis absorption, photoluminescence, and step−scan time-resolved infrared were used to interrogate the photophysical behavior of **1**, ultimately revealing a long-lived excited state characteristic of ^{3}IL PDI parentage. The transient infrared signatures of the ^{3}PDI localized excited state have been evaluated for the first time and found to correlate well with the corresponding DFT calculations.

RESULTS AND DISCUSSION

Syntheses. The PDI-based synthetic precursors **3** and **4** were prepared using procedures previously reported in the literature.[94,99] The Pt[(^{t}Bu$_3$tpy)Cl]PF$_6$ metal complex precursor was synthesized according to a published procedure using Pt(DMSO)$_2$Cl$_2$[100] and commercially available 4,4′,4″-tri-*tert*-butyl-2,2′:6′,2″-terpyridine (^{t}Bu$_3$tpy).[101] The metal−organic chromophores **1** and **2** were synthesized using established literature protocols, namely, Cu(I)-catalyzed cross-coupling reactions between the Pt(II) halide precursor and **4** in the presence of diisopropylamine in dichloromethane at room temperature under an inert atmosphere.[57,58,94] We note that this particular coupling reaction also readily proceeds without addition of Cu(I), as has been previously noted.[57] This latter approach affords the opportunity to completely avoid possible π-complex formation with Cu(I) to the resulting metal−carbon acetylide bond in the final isolated Pt(II) complex. As a result, complications associated with purification and subsequent characterization by MALDI-TOF MS and FT-IR spectroscopy are completely circumvented.[102,103] The final isolated metal complexes were structurally characterized by ^{1}H NMR, MALDI-TOF MS, high-resolution ESI-MS, and FT-IR. Molecules **1** and **2** are stable in the solid state and solution under ambient conditions and soluble in a variety of solvents including dichloromethane, methanol, 2-methyltetrahydrofuran (2-MeTHF), and toluene.

Electronic Absorption Spectroscopy. The UV−vis absorption spectra of **1** in various solvents are displayed in Figure 1a whose peaks and extinction coefficients are summarized in Table 1. The intense transitions near 325 nm ($\varepsilon \approx 30\,000-33\,000$ M^{-1} cm^{-1}) correspond to $\pi-\pi^*$ transitions of the ^{t}Bu$_3$tpy ligand as previously reported.[57,58,101]

The lower energy transitions observed in the 400−600 nm range ($\varepsilon \approx 17\,700-49\,500$ M^{-1} cm^{-1}) are attributed to $\pi-\pi^*$ transitions of the PDI acetylide moiety in addition to characteristic Pt(II)−acetylide to ^{t}Bu$_3$tpy charge-transfer transitions.[94,95] The latter is supported by comparing the integration of the absorption spectra of **1** and **4**, which produces a 1.4:1 ratio, Figure S1, Supporting Information. This signifies the presence of additional CT transitions obscured by the intense $\pi-\pi^*$ transitions localized on the PDI moiety. The PDI-centered $\pi-\pi^*$ transitions of **1** are shifted to significantly lower energies in comparison to the free ligand **4**, likely resulting from strong σ donation accompanied by π back bonding from the Pt(II) metal center, Figure S1, Supporting Information.[77,94,95,104] Additionally, the absence of a significant solvatochromic effect in the absorption spectrum of **1**, as shown in Figure 1a, supports the notion that the majority of the oscillator strength in the low-energy visible portion of the spectrum is due to ligand-localized PDI acetylide-based transitions. In all solvents, the absorption spectral profile of **1** was independent of chromophore concentration. In contrast with the other solvents measured, in toluene the PDI acetylide-based $\pi-\pi^*$ transitions display a decrease in the ratio of the oscillator strengths in the two lowest energy transitions (I_{0-0}/I_{1-0}) as well as a red shift in the 0−0 transition, Figure 1a. This difference in vibronic structure is a characteristic signature of PDI aggregate formation, which is known to occur in toluene.[105] Upon addition of a polar solvent (methanol) to solutions of **1** in toluene, the molecules deaggregate and the resulting spectrum becomes identical to all other solvents investigated, Figure S2, Supporting Information.

Static and Time-Resolved Photoluminescence. Unlike the previously reported nonluminescent Pt(II) bipyridyl bis(PDI−acetylides),[94,95] **1** displays easily detectable red emission in both aerated and degassed solutions with

dx.doi.org/10.1021/ic301169t | Inorg. Chem. 2012, 51, 8589−8598

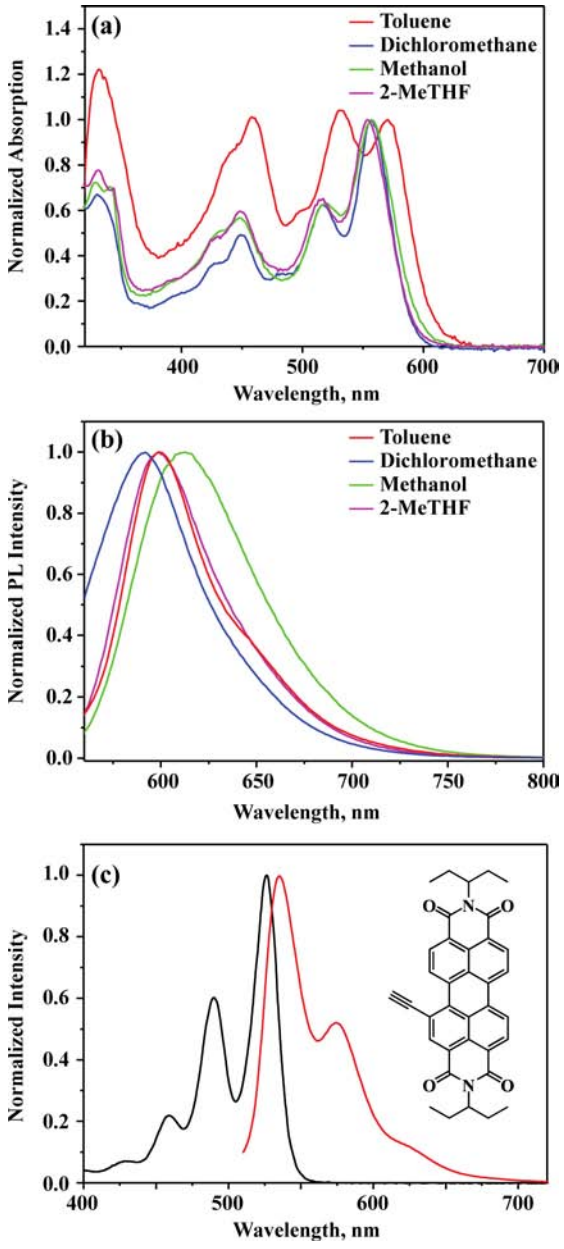

Figure 1. (a) Absorption and (b) photoluminescence (λ_{ex} = 540 nm) spectra of **1** in various solvents at 298 K. (c) Absorption (black) and photoluminescence (red) (λ_{ex} = 490 nm) spectra of **4** in 2-methyltetrahydrofuran at 298 K.

correspondingly small Stokes shifts, Figure 1b. No quenching of emission intensity was observed upon saturation of samples with air, suggesting that the photoluminescence originates from a singlet excited state. Comparison of the emission spectra at 298 and 77 K in 2-MeTHF, Figure S3, Supporting Information, revealed only a minor thermally induced Stokes shift (ΔE_s = E_{em}(77 K) − E_{em}(298 K) = 611 cm^{-1}). This is consistent with little charge redistribution between ground and excited states and is therefore assigned as PDI-acetylide-localized singlet fluorescence. Addition of methanol to solutions of **1** in toluene, where the molecules are initially aggregated, shows no influence on the resultant emission spectrum band shape; only a slight red shift is observed due to solvent stabilization effects, Figure S4, Supporting Information. This implies that the emission is occurring from the nonaggregated state in all solvents. The fluorescence quantum yield (Φ = 0.014 ± 0.001) and lifetime (τ = 109 ps) of **1** in dichloromethane are significantly reduced compared to the "free" PDI acetylene precursor **4**, where Φ = 0.91 and τ = 4.5 ± 0.1 ns, Figures S5 and S6, Supporting Information. This indicates that although singlet fluorescence is observed from **1**, it is enormously quenched with respect to the free ligand. This implies that intersystem crossing to the corresponding triplet is likely occurring, similar to that observed in the bipyridyl and phosphine-supported Pt(II) PDI−acetylides.[94,95] Formation of the triplet state in **1** was indirectly supported by the observation of singlet oxygen ($^1O_2$) photoluminescence at ∼1275 nm upon excitation of aerated solutions at 450 nm, Figure S7, Supporting Information. Production of singlet oxygen was observed in air-saturated 2-MeTHF, methanol, toluene, and acetonitrile, ultimately quantified in the latter (Φ = 0.52 ± 0.05).[106] No phosphorescence from **1** was observed in either the visible or the near-IR region of the spectrum at room temperature or 77 K, in complete agreement with previously reported non-phosphorescent Pt(II) bis(PDI-acetylide) complexes, including the phosphine model complex **2**.[94,95]

Electrochemistry. The cyclic voltammograms (CVs) and differential pulse voltammograms (DPVs) measured for **1** in argon-saturated dichloromethane containing 0.1 M tetrabutylammonium hexafluorophosphate ($TBAPF_6$) as the supporting electrolyte exhibit three reversible reductions and one irreversible oxidation, Figures 2 and S8, Supporting Information. The electrochemical potentials are reported versus the $Fe(Cp)_2^{+/0}$ external standard ($E_{1/2}$ = 0.44 V vs Ag/AgCl) and are summarized in Table 1. The first two reversible reductions occurring at −1.04 and −1.26 V are assigned as two sequential one-electron reductions of the PDI unit by comparison to the previously reported reduction potentials for **4** (−1.03 and

Table 1. Photophysical and Electrochemical Properties of 1

λ_{abs}[a]/nm (ε, M^{-1} cm^{-1})	λ_{em}[b]/nm	τ_{em}[a]/ps	Φ_{em}[a,d]	$E_{1/2}^{ox}$/V[a,e,f]	$E_{1/2}^{red}$/V[a,e,g]	Φ ($^1O_2$)[h]
557 (49 500)	600[c]/607[d]	109 ± 10	0.014 ± 0.001	+1.05	−1.04	0.52 ± 0.05
517 (31 000)					−1.26	
450 (24 500)					−1.46	
425, sh (17 700)						
330 (33 300)						
316 (30 900)						

[a]Measured in dichloromethane. [b]Measured in 2-MeTHF. [c]Determined in a conventional fluorimeter, ±2 nm. [d]Determined using an absolute quantum yield apparatus, ±2 nm. [e]Electrochemical potential peaks measured by DPV with $TBAPF_6$ as supporting electrolyte (0.1 M), reported vs $Fe(Cp)_2^{+/0}$ couple. [f]Irreversible process, as determined by CV. [g]Reversible process, as determined by CV. [h]Singlet oxygen quantum yield measured in air-saturated acetonitrile relative to $[Ru(bpy)_3](OTf)_2$ (Φ = 0.57 ± 0.05).[106]

dx.doi.org/10.1021/ic301169t | Inorg. Chem. 2012, 51, 8589−8598

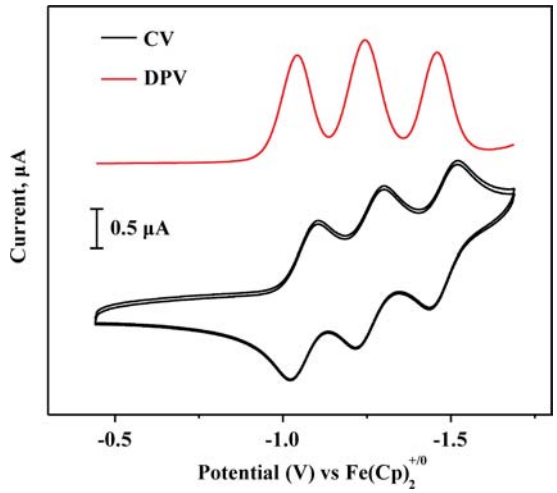

Figure 2. Cyclic and differential pulse voltammograms for reduction of **1** in an argon-saturated 0.1 M solution of $TBAPF_6$ in dichloromethane.

−1.24 V vs $Fe(Cp)_2^{+/0}$).[95] The third reduction at −1.46 V is assigned as a one-electron reduction of the terpyridyl ligand by comparison to previously reported Pt(II) terpyridyl acetylide complexes.[58] The irreversible anodic wave at 1.05 V appears as removal of an electron, presumably from the PDI-acetylide subunit as suggested by the ligand-localized nature lowest energy transition in the absorption spectrum, Figure 1a. However, we cannot rule out that this irreversible oxidation might indeed be metal centered in **1**. Consistent with our assignment, DFT calculations performed on **1** (Figure S9, Supporting Information) indicate that both the HOMO and the LUMO (and energetically proximate) orbitals are predominantly PDI-acetylide localized, supporting the idea that the observed oxidation likely corresponds to removal of an electron from a PDI-based orbital.

Nanosecond Transient Absorption Spectroscopy. Transient absorption difference spectra of **1** were acquired in an argon-saturated flow cell following 555 nm pulsed laser excitation (fwhm ≈ 5−7 ns, 2 mJ/pulse, Nd:YAG/OPO laser) in toluene and 2-MeTHF at room temperature, Figure 3. The resulting difference spectra in both solvents display identical bleaching and absorption features except for a slight red shift of all bands in the case of toluene, where the molecules are aggregated. This red shift of the transient absorption spectrum in toluene is consistent with the red shift observed in the ground-state absorption spectrum, suggesting that the transient absorption is probing the aggregated form. In 2-MeTHF, **1** exhibited ground-state bleaches centered at 320 and 555 nm, along with an intense excited-state absorption band centered at 490 nm and a minor broad positive absorption band in the red. These transient absorption features together with the long excited-state lifetime in 2-MeTHF (372 ns) are in excellent agreement with previously reported ^{3}IL PDI transient absorption difference spectra and lifetimes in the analogous bipyridyl and phosphine-supported Pt(II) bis(PDI−acetylide).[94,95] Similar transient features were generated in toluene, Figures 3 and S10, Supporting Information, and the data here were also adequately modeled using first-order kinetics (τ = 503 ns). Additionally, no features corresponding to the ^{1}PDI state, charge-transfer triplet states (^{3}MLCT or ^{3}LLCT), or PDI-based radical cation or anion were observed in the transient absorption difference spectra of **1** at all delay times within our experimental window.[36,57,95,107−110] Finally, the excited-state

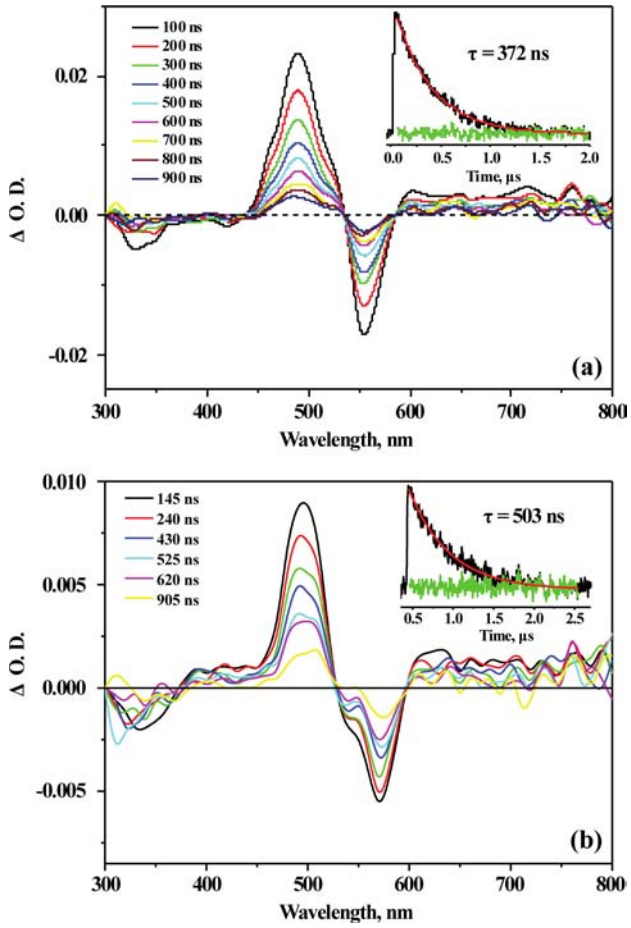

Figure 3. Transient absorption difference spectra of **1** in 2-MeTHF (a) and toluene (b) following 555 nm pulsed laser excitation (2 mJ/pulse, 5−7 ns fwhm) measured at the delay times specified. (Insets) Single-wavelength (λ_{obs} = 490 nm) transient absorption decays with their corresponding single-exponential fits (red) and the resulting residuals (green) illustrating adequate goodness of fit. Each difference spectrum represents the average of 64 measurements.

absorption features displayed by **1** are qualitatively similar to transient absorptions reported for bimolecular-sensitized PDI triplet state, wherein the $T_1 \rightarrow T_n$ transitions generally occur to the blue of the strongest singlet ground-state absorption.[94,111] Similarly, the ground-state bleach is without question completely associated with the PDI subunit, strongly suggesting that the singlet depletion on long time scales is a result of triplet-state formation. The single-exponential kinetics exhibited by the transient absorption decays of **1** were identical across the entire spectrum for both solvents investigated. Overall, the transient absorption data presented here leave little doubt that the lowest excited state is localized on the PDI moiety **1** and triplet in nature.

Static and Step−Scan Time-Resolved FT-IR Spectroscopy. Time-resolved infrared (TRIR) spectroscopy is another useful tool for identification and characterization of excited states. Although it is far less accessible than UV−vis transient absorption spectroscopy, in metal complexes that have strong infrared active groups such as cyanides, carbonyls, or amides, TRIR spectrsocopy has proven to be a valuable tool in characterizing the nature of long-lived excited states,[112−115] identifying electron- or energy-transfer products,[116,117] and probing reaction products and intermediates.[118,119] This

dx.doi.org/10.1021/ic301169t | Inorg. Chem. 2012, 51, 8589−8598

spectroscopic technique has previously been applied to metal complexes of the related 4-piperidinyl-1,8-naphthalimide (PNI) chromophore to probe the long-lived ^{3}IL PNI state.[114,115,119] As the PDI acetylide chromophore is rich in distinctive infrared-active C═O, C≡C, and aromatic C═C vibrations, the excited states of **1** were investigated by time-resolved FT-IR spectroscopy in dichloromethane solution, which is transparent in the relevant mid-IR window.

Figure 4 presents the FT-IR spectra of **1**−**3** in dichloromethane solution. The FT-IR spectrum of **1** can be readily

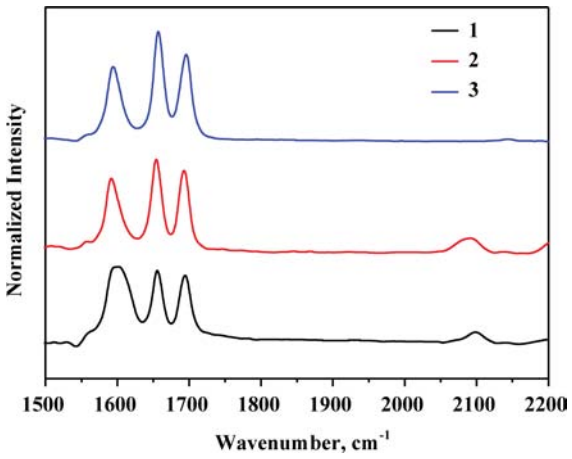

Figure 4. FT-IR spectra of **1**−**3** in dichloromethane.

assigned by direct comparison to **3**, which contains vibrations characteristic of the PDI portion of the complex (Figure 4, Table 2), namely, two peaks at 1695 and 1657 cm^{-1} due to the vibrations of the C═O groups and a peak at 1598 cm^{-1} resulting from various vibrations of the PDI aromatic core, all in excellent agreement with previously reported spectra of the closely related 1,4,5,8-naphthalenediimide[120] and PNI.[114,115] The oscillator strength of the C≡C bond in **3** is too low to be observed in its FT-IR spectrum in solution. Similarly, **2** exhibits nearly identical infrared-active stretches emanating from the PDI acetylide moiety (Figure 4, Table 2), including a C≡C vibration at 2091 cm^{-1}, two C═O bands centered at 1692 and 1655 cm^{-1}, and delocalized PDI aromatic core vibrations at 1590 cm^{-1}. Collectively, **1** and **2** exhibit nearly identical IR spectroscopic signatures (Figure 4 and Table 2) differing only in their respective aromatic rings stretches that are broadened due to the additional contribution of terpyridyl moiety vibrations in **1**. The relative intensities of the vibrations that arise from the PDI acetylide unit in **1** are reduced in comparison with **2**, consistent with having only one PDI acetylide subunit in the former.

Before proceeding with the discussion it is important to note that the lifetimes of the TRIR absorption features measured for **1** and **2** (τ = 286 and 660 ns, respectively, Figures S11 and S12, Supporting Information) are on the same order of those observed in the transient absorption kinetics, strongly suggesting that the same excited state is being probed in each spectroscopic domain. In the TRIR difference spectrum of **1** measured 50 ns after a 532 nm laser pulse, Figure 5, the C═O

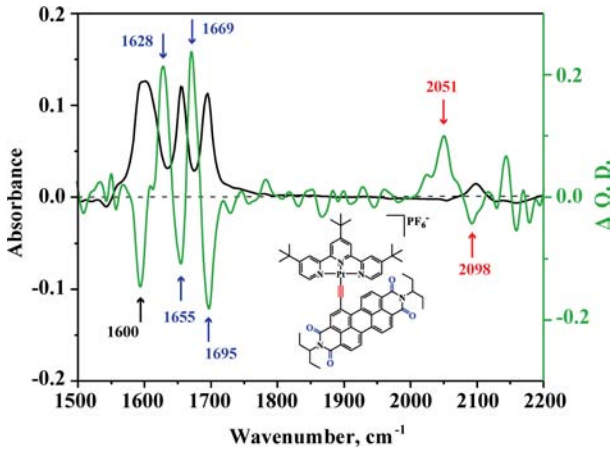

Figure 5. Ground-state FT-IR spectrum (black) and time-resolved step−scan FT-IR difference spectrum (green) of **1** in dichloromethane at 50 ns delay following 532 nm pulsed excitation. Measurements were performed in a 1 mm path length CaF_2 cell purged with argon at a spectral resolution of 8 cm^{-1}.

and C≡C vibrations have all shifted to lower energy upon promotion to the long-lived excited state ($\Delta E \approx$ 30−50 cm^{-1}, Table 2). The combined data are consistent with a net lowering of the C≡C and C═O bond order upon sensitization of the ^{3}PDI excited state, and importantly, the observed red shifts in the C═O frequencies are on the order of those observed in the related PNI-containing metal−organic chromophores.[114,115] The TRIR difference spectrum of **2** (Figure 6) measured at the same delay time is nearly identical to that of **1**, namely, the C≡C and C═O vibrations are all shifted to lower energy by ∼30−50 cm^{-1}, Table 2, consistent with production of a ^{3}PDI-localized excited state on a *single* PDI−acetylide subunit. It is important to note that the model complex **2**, whose lowest energy excited state has previously been assigned as ^{3}PDI-acetylide localized in nature, contains two equivalent PDI-acetylide ligands, and the resulting excited state could potentially be either localized on a single PDI or delocalized

Table 2. Experimental and Calculated Vibrational Energies in the Ground and Lowest Triplet Excited States of 1−3 in Dichloromethane

	1			2			3			
vibrations	GS,[a] cm^{-1}	TR,[a] cm^{-1}	ΔE, cm^{-1}	GS,[a] cm^{-1}	TR,[a] cm^{-1}	ΔE, cm^{-1}	GS,[a] cm^{-1}	GS,[b] cm^{-1}	TS,[b] cm^{-1}	ΔE, cm^{-1}
C≡C	2098	2051	−47	2091	2041	−50		2152	2114	−38
C═O(s)	1695	1669	−26	1692	1669	−23	1695	1684[c]	1654[c]	−30
C═O(a)	1655	1628	−27	1655	1628	−27	1657	1641[c]	1613[c]	−28

[a]Time-resolved FT-IR spectroscopy at a spectral resolution of 8 cm^{-1}. [b]DFT frequency calculations performed with the UB3LYP/6-31g(d) functional/basis in dichloromethane dielectric field, reduced by a generic frequency scaling factor of 0.9613. [c]Average of two closely spaced vibrations: s, symmetrical; a, asymmetrical. ΔE is the difference between GS (ground state) and TS (calculated triplet state) or TR (time-resolved) triplet state.

dx.doi.org/10.1021/ic301169t | Inorg. Chem. 2012, 51, 8589−8598

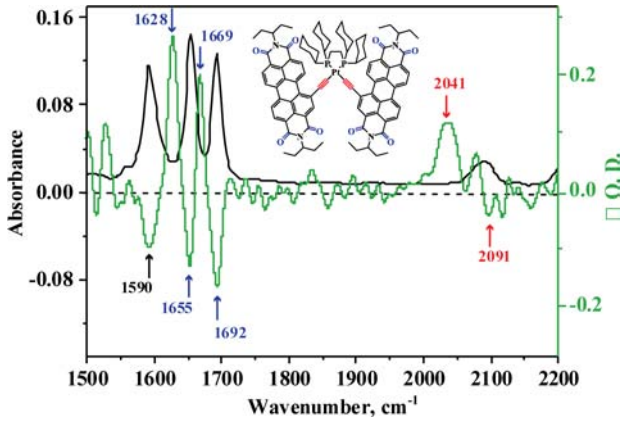

Figure 6. Ground-state FT-IR spectrum (black) and time-resolved step−scan FTIR difference spectrum (red) for **2** in dichloromethane at 50 ns delay following 532 nm pulsed excitation. Measurements were performed in a 1 mm path length CaF_2 cell purged with argon at a spectral resolution of 8 cm^{-1}.

over both. Given the fact that the TRIR data are nearly identical and result in red shifts of the same magnitude, the excited state in **2** must be localized on a single PDI acetylide unit. Otherwise, if the excited state was delocalized over both PDI acetylide ligands in **2**, the magnitude of the shifts in the TRIR spectrum would likely be about one-half of those observed in the TRIR spectrum of **1**.[112]

In order to obtain more detailed information regarding the nature of the observed peaks in the ground state and TRIR difference spectra, DFT calculations were performed on the purely organic **3** using previously described computational methods.[114,121] Given significant difficulties with excited-state calculations on **1**, which never properly converged, we had no choice but to attempt to correlate the DFT-calculated frequencies from **3** and compare these to **1**. The frequencies of the geometry-optimized ground (singlet) and lowest energy triplet states were calculated in a simulated dichloromethane solvent environment whose values are collected in Table 2. All reported frequencies were scaled by 0.9613, the correction factor appropriate for the functional and basis set used.[121] The calculated ground-state frequencies correlate well with both the experimental FT-IR spectrum as well as the calculated frequencies on previously reported PDI systems.[121] The calculations illustrate that because of the low symmetry inherent in **3**, the two carbonyl bands observed in the experimental spectrum are each composed of two closely spaced vibrations, the higher energy band being composed of symmetric vibrations and the lower energy band being composed of asymmetric vibrations. The calculated infrared spectrum, Figure S13, Supporting Information, also shows that the lowest energy band near 1570 cm^{-1} is composed of many different aromatic-based stretching frequencies. In agreement with experiment, the calculated ground-state infrared spectrum of **3** indicates that the C≡C vibration is of very low intensity and cannot be readily observed. The calculated infrared spectrum of the lowest energy triplet state of **3**, Figure S14, Supporting Information, produces a red shift of both the C≡C and the C═O vibrational frequencies, −38 cm^{-1} for the C≡C and −28 and −30 cm^{-1} for the two C═O bands, with respect to the ground-state singlet frequencies. These shifts agree well with the magnitude of those seen in the TRIR spectra of **1** and **2** in dichloromethane. The lone aromatic peak observed in the calculated ground-state spectrum of **3** splits into many low-intensity vibrations, all at lower energy, in the calculated lowest energy triplet spectrum. Overall, the DFT calculations performed on the purely organic model chromophore **3** are in excellent agreement with the TRIR experiments on metal complexes **1** and **2** and consistent with formation of a ^{3}PDI acetylide-localized excited state.

CONCLUSIONS

A comprehensive photophysical study has been performed on a Pt(II) terpyridyl perylenediimideacetylide complex (**1**) revealing the spectroscopic characteristics of its associated ligand-localized triplet state in both transient absorption and time-resolved step-scan FT-IR, the latter for the first time. The transient absorption difference spectrum was nearly identical to that measured in the phosphine-supported Pt(II) model PDI−acetylide complex **2**, possessed a strong singlet state bleach of the PDI ground-state absorption and a strong transient signal located immediately to the blue, and both triplets exhibited similar excited-state lifetimes. Correspondingly, the transient IR signals from **1** also correlated well with that observed in **2** and possessed excited-state lifetimes similar to that measured in the transient absorption experiments. In both cases, the relevant vibrations red shifted in the excited state, consistent with ligand-localized triplet-state formation in addition to the associated DFT calculations performed on the singlet and lowest triplet states on the nonmetalated PDI model **3**. Finally, the ligand-localized PDI triplet state in **1** successfully sensitized formation of $^1O_2$ in aerated solutions with reasonably high efficiency, $\Phi(^1O_2) = 0.52$, but displayed no phosphorescence at 298 or 77 K.

EXPERIMENTAL SECTION

Reagents and Chemicals. All precursors, solvents, and reagents were commercially available and used as received. Silica gel (SI 60, particle size 40−63 μm) for stationary phase in column chromatography was purchased from VWR International. Aluminum oxide (activated, neutral, Brockmann I) for stationary phase in column chromatography was purchased from Sigma-Aldrich.

General. ^{1}H NMR spectra were recorded on a Bruker Avance 300 (300 MHz) or a Bruker Avance 500 (500 MHz) spectrometer. The resulting free induction decay (FID) data was processed with MestReNova 7.1.2. All chemical shifts are referenced to tetramethylsilane (TMS) as internal standard, and splitting patterns are assigned as s (singlet), d (doublet), t (triplet), q (quartet), and m (multiplet). ^{31}P NMR spectra were obtained on a Varian Unity INOVA 400 MHz spectrometer, and chemical shifts were referenced to external 85% H_3PO_4. Mass spectra were measured using a Shimatzu GCMS spectrometer (QP5050A). MALDI-TOF spectra were measured with a Bruker-Daltonics Omniflex spectrometer. High-resolution electrospray MS spectra were obtained at the Michigan State University Mass Spectrometry Facility.

Syntheses. Compounds **2**,[94] **3**,[94,99] and **4**[94] were synthesized according to literature procedures and yielded satisfactory mass and ^{1}H NMR spectra. [Pt(^{t}Bu$_3$tpy)Cl]PF_6 (where ^{t}Bu$_3$tpy is 4,4′,4″-tri-*tert*-butyl-2,2′:6′,2″-terpyridine) was synthesized according to the adopted procedure.[101]

[Pt(^{t}Bu$_3$tpy)CCPDI]PF_6 (1). [Pt(^{t}Bu$_3$tpy)CCPDI]PF_6 (**1**, where PDI = *N*,*N*′-bis(ethylpropyl)perylene-3,4:9,10-tetracarboxylic diimide) was synthesized by adapting an existing procedure.[94] Under an atmosphere of nitrogen in a glovebox, [Pt(^{t}Bu$_3$tpy)Cl]PF_6 (42 mg, 0.050 mmol), PDI acetylene (**4**) (30 mg, 0.054 mmol), CuI (2 mg), and 6 mL of *i*-Pr_2NH were stirred in CH_2Cl_2 at room temperature for 24 h. The solvent was evaporated under vacuum, and crude product was purified by column chromatography (1 vol % methanol in CH_2Cl_2, alumina oxide) to afford dark purple crystals (30 mg, 46%).

dx.doi.org/10.1021/ic301169t | Inorg. Chem. 2012, 51, 8589−8598

^{1}H NMR (500 MHz, $CDCl_3$), δ: 10.89 (d, 1H, J = 8.2 Hz), 9.19 (d, 2H, J = 6.0 Hz), 8.89 (s, 1H), 8.72−8.61 (m, 4H), 8.62 (d, 1H, J = 8.2 Hz), 8.30 (s, 2H), 8.26 (d, 2H, J = 2.0 Hz), 7.69 (dd, 2H, J = 6 Hz and J = 2 Hz), 5.12−5.05 (m, 2H), 2.33−2.23 (m, 4H), 2.01−1.90 (m, 4H), 1.60 (s, 9H), 1.52 (s, 18H), 0.95 (t, 6H, J = 7.4 Hz), 0.93 (t, 6H, J = 7.5 Hz). MALDI-TOF MS: m/z = 1150.51 $[M - PF_6]^+$. ESI-HRMS found: 1149.4626 $[M - PF_6]^+$, $C_{63}H_{64}N_5O_4{}^{195}Pt$ requires 1149.4606.

Photophysical Measurements. Spectroscopic-grade solvents purchased from Sigma-Aldrich without further purification were used for photophysical measurements. Steady-state absorption spectra were measured with a Varian Cary 50 UV−vis spectrophotometer, accurate to ±2 nm. Uncorrected steady-state photoluminescence spectra were measured with Edinburg and Hamamatsu spectrofluorimeters. An Edinburgh fluorimeter (FS920) was equipped with a Peltier-cooled single-photon counting photomultiplier detection system (R2658P) or a Hamamatsu NIR photomultiplier (PMT) module (H10330A-75, InP/InGaAs) operating at −700 V (forced air cooling), Czerny-Turner monochromators (excitation, emission) with a 1800 g mm $^{-1}$ grating blazed at 500, 750, or 1200 nm, and a 450 W xenon arc lamp (Xe900) as an excitation source operating under control of F900 software from Edinburgh. Spectra were recorded with a 550 nm long-path filter. Photoluminescence quantum yields were measured with a Hamamatsu absolute quantum yield system (Quantaurus-QY C11347-11) equipped with a 150 W xenon lamp and multichannel detector (CCD sensor), accurate to less than ±2 nm. The resulting values represent the average of three measurements. Absorption and emission measurements were performed in a 1 cm^2 quartz cell (Starna Cells) using optically dilute (OD = 0.09−0.11) solutions. Samples for steady−state and time-resolved photoluminescence spectroscopy were degassed by the freeze−pump−thaw technique (at least 3 cycles).

77 K Static Photoluminescence. Steady-state photoluminescence spectra at 77 K in the visible and NIR regions were recorded by the Edinburgh fluorimeter (FS920) described above. Photoluminescence profiles in the visible range were acquired with a Peltier-cooled single-photon counting photomultiplier detection system (R2658P). The NIR range was scanned with a Hamamatsu NIR photomultiplier (PMT) module (H10330A-75, InP/InGaAs) operating at −700 V (forced air cooling). Temperature control was achieved with a temperature controller (Oxford, ITC503) connected to an OptistatDN variable-temperature liquid nitrogen cryostat (Oxford).

Nanosecond Transient Absorption Spectroscopy. Nanosecond transient absorption spectra in the visible and NIR range were collected with a spectrometer that has been described previously.[95] A Proteus spectrometer (Ultrafast Systems) was equipped with a 150 W Xe arc lamp (Newport), a Bruker Optics monochromator, with two diffraction gratings blazed for visible and near-IR dispersion, and Si or InGaAs photodiode detectors (Thorlabs, DET 10A and DET 10C) optically coupled to the exit slit of the monochromator. Measurements were performed at ambient temperature in a 1 cm^2 quartz flow cell purged with high-purity argon during the experiment, and an absorbance of 0.4 at the excitation wavelength. The average of 128 measurements were collected following 555 nm excitation from a computer-controlled Nd:YAG laser/OPO system (Opotek, Vibrant LD 355 II) with 2 mJ/pulse power and a repetition rate of 10 Hz. Resulting data were analyzed with Origin 8.6 software.

Nanosecond transient absorption spectra in the UV−vis region were collected with a commercial laser flash photolysis spectrometer (LP920-K, Edinburgh Instruments) equipped with a pulsed 450 W ozone-free Xe arc lamp (Xe900), symmetrical Czerny-Turner monochromator (TMS300) with a 1800 g mm^{-1} grating, blazed at 500 nm. The signal from the PMT detector (Hamamatsu, R928) was recorded on a 100 MHz oscilloscope (TDS3012C). Measurements were performed at ambient temperature in a 1 cm^2 quartz cell. All solutions had an absorbance of 0.4 at the excitation wavelength and were degassed by the freeze−pump−thaw technique (at least three cycles) before measuring. The average of 64 measurements was collected following 555 nm excitation pulses from a computer-controlled Nd:YAG laser/OPO system (Opotek, Vibrant LD 355 II) with a 2 mJ/pulse power and repetition rate of 1 Hz. The resulting data were analyzed with Origin 8.6 software.

Nanosecond Step−Scan Infrared Spectroscopy. Nanosecond time-resolved step−scan FT-IR absorption spectra were measured on a step−scan-modified Bruker Vertex 70 FT-IR spectrometer with a standard globar source. Compounds were dissolved in dichloromethane to give a ground-state infrared absorption of >0.1 for the carbonyl bands. All solutions were deoxygenated by bubbling with high-purity argon for 20 min. Spectra were measured at ambient temperature in a demountable CaF_2 cell with a 1 mm Teflon spacer (Specac). Samples were excited using the 532 nm second-harmonic output of a Nd:YAG laser (Continuum Surelite I) laser (∼7 mJ/pulse, ∼2 cm diameter spot, 10 Hz). An ac/dc-coupled photovoltaic Kolmar Technologies mercury cadmium telluride (PV MCT) detector with a 20 MHz preamplifier was used to sample the transmitted IR probe beam. The detector's ac signal was further amplified (10×) with a 100 MHz fast preamplifier (FEMTO DHPVA) before being directed to a 400/250 MHz M3i.4142 transient digitizer board. The interferogram response before and after laser excitation was collected in 25 ns time slices, with 20 laser shots averaged at each mirror position. Long- and short-pass filters (Spectragon) were used to isolate the spectral region of interest. For each scan, folding limits of 2400 and 1300 cm^{-1} at 8 cm^{-1} resolution resulted in 512 mirror positions. The dc signal was collected separately and used to check for sample decomposition as well as for phase correction of the ac signal. Bruker Instruments' Opus 7.0 software was used to process the recorded data. Differential absorbance spectra were calculated from the ac and dc single-channel spectra as described previously.[122] The differential excited-state absorption spectra reported herein represent an average of 10 scans (**1**) or 5 scans (**2**), and ground-state spectra correspond to an average of 32 (rapid) scans.

Singlet Oxygen Sensitization. Singlet oxygen formation quantum yield measurements were performed in aerated solutions of acetonitrile in a 1 cm^2 quartz cell at ambient temperature with the Edinburgh fluorimeter (FS920) and NIR PMT described above. The resulting value is an average of three measurements relative to $[Ru(bpy)]_3(OTf)_2$ (Φ = 0.57 ± 0.05) in air-saturated acetonitrile and 450 nm excitation wavelength.[106] The singlet O_2 quantum yield was calculated as previously described.[94]

Time-Resolved Photoluminescence Techniques. Fluorescence lifetime measurements were performed by the time-correlated single-photon counting (TCSPC) technique on an Edinburgh spectrometer (LifeSpec II) equipped with a microchannel plate photomultiplier tube (Hamamatsu R3809U-50). Lifetime decays were obtained followed by excitation from a Coherent Ti:Sapphire laser (Chameleon Ultra II) with power monitored by a Molectron Power Max 5200 power meter. For complex **1** lifetime decay measurement, laser wavelength was tuned to 900 nm, pulse picked through a 4 MHz Coherent 9200 pulse picker, and frequency doubled by an APE-GmbH SHG (second-harmonic generator) unit to produce a 450 nm laser beam (5 mW). For PDI acetylene (**4**) lifetime decay measurement, laser wavelength was tuned to 920 nm, pulse picked through a 4 MHz Coherent 9200 pulse picker, and frequency doubled by an APE-GmbH SHG (second-harmonic generator) unit to produce a 460 nm laser beam (3 mW). Measurements were performed in a 1 cm^2 quartz cell (Starna Cells) using optically dilute (OD = 0.09−0.11) solutions. Instrument response function was collected using a dilute solution of Ludox at 450 nm excitation wavelength. Reconvolution of the fluorescence decay and instrument response function together with lifetime fitting of complex **1** was performed on the Edinburgh software (F900). Tail fit of the photoluminescence lifetime decay of **4** was performed by Origin 8.6 software.

Electrochemistry. Electrochemical measurements were performed in dichloromethane solutions with 0.1 M $TBAPF_6$ as the supporting electrolyte at room temperature, with a platinum disk as the working electrode, platinum wire as the counter electrode, and Ag/AgCl (3 M NaCl) as the reference electrode. Solutions were saturated with argon prior to each measurement. The ferrocenium/ferrocene couple ($FeCp_2^{+/0}$) was used as an external reference for all measurements, and potentials are reported relative to $FeCp_2^{+/0}$. The cyclic and

dx.doi.org/10.1021/ic301169t | Inorg. Chem. 2012, 51, 8589−8598

differential pulse voltammograms were recorded with a Bioanalytical Systems Epsilon potentiostat interfaced with a Pentium PC.

DFT Calculations. Calculations on **1** and **3** were performed using the Gaussian 09 software package[123] and the computational resources of the Ohio Supercomputer Center. Geometry optimization of the ground state of **1** was performed using the B3LYP functional and LANL2DZ basis set. Geometry optimizations on **3** were done on both the ground state and the lowest energy triplet state using the UB3LYP functional and 6-31g(d) basis set.[114,121] No symmetry restrictions were placed on the geometry optimizations. The polarizable continuum model (PCM) was used to simulate the effects of the dichloromethane solvent environment. Frequency calculations were performed on all optimized structures to ensure that these geometries corresponded to global minima. No imaginary frequencies were obtained for any of the optimized geometries. For comparison to the experimental values, the calculated frequencies of **3** were scaled by a factor of 0.9613, the reported correction factor for the functional and basis set used.[121] HOMO and LUMO orbitals of **1** and **3** and spin density of the lowest energy triplet state of **3** were visualized using GaussView 5.

■ ASSOCIATED CONTENT

Ⓢ Supporting Information

Additional time-resolved, steady-state, and calculated spectra of **1**−**4**, HOMO and LUMO orbital isodensity plots for **1** and **3**, and ^{1}H NMR characterization of **1**. This material is available free of charge via the Internet at http://pubs.acs.org.

■ AUTHOR INFORMATION

Corresponding Author

*E-mail: castell@bgsu.edu.

Notes

The authors declare no competing financial interest.

■ ACKNOWLEDGMENTS

This research was supported by the National Science Foundation (CHE-1012487), the Air Force Office of Scientific Research (FA9550-05-1-0276), and the BGSU Research Enhancement Initiative. The authors thank Dr. Mykhaylo Myahkostupov, Dr. Sebastien Goeb, and Dr. Aaron A. Rachford for their valuable suggestions. High-resolution electrospray MS experiments were performed at the Michigan State University Mass Spectrometry Facility.

■ REFERENCES

(1) Chung, C. Y. S.; Yam, V. W. W. *J. Am. Chem. Soc.* **2011**, *133*, 18775−18784.
(2) Wong, K. M. C.; Yam, V. W. W. *Acc. Chem. Res.* **2011**, *44*, 424−434.
(3) Lo, H. S.; Yip, S. K.; Zhu, N.; Yam, V. W. W. *Dalton Trans.* **2007**, 4386−4389.
(4) Tam, A. Y. Y.; Wong, K. M. C.; Wang, G. X.; Yam, V. W. W. *Chem. Commun.* **2007**, 2028−2030.
(5) Yam, V. W. W.; Chan, K. H. Y.; Wong, K. M. C.; Zhu, N. *Chem.—Eur. J.* **2005**, *11*, 4535−4543.
(6) Field, J. S.; Haines, R. J.; McMillin, D. R.; Munro, O. Q.; Summerton, G. C. *Inorg. Chim. Acta* **2005**, *358*, 4567−4570.
(7) Yam, V. W. W.; Wong, K. M. C.; Zhu, N. *J. Am. Chem. Soc.* **2002**, *124*, 6506−6507.
(8) Lu, W.; Chen, Y.; Roy, V. A. L.; Chui, S. S. Y.; Che, C. M. *Angew. Chem., Int. Ed.* **2009**, *48*, 7621−7625.
(9) Leung, S. Y. L.; Tam, A. Y. Y.; Tao, C. H.; Chow, H. S.; Yam, V. W. W. *J. Am. Chem. Soc.* **2012**, *134*, 1047−1056.
(10) Yu, C.; Wong, K. M. C.; Chan, K. H. Y.; Yam, V. W. W. *Angew. Chem., Int. Ed.* **2005**, *44*, 791−794.
(11) Yeung, M. C. L.; Wong, K. M. C.; Tsang, Y. K. T.; Yam, V. W. W. *Chem. Commun.* **2010**, *46*, 7709−7711.
(12) Chung, C. Y. S.; Chan, K. H. Y.; Yam, V. W. W. *Chem. Commun.* **2011**, *47*, 2000−2002.
(13) Chan, K. H. Y.; Chow, H. S.; Wong, K. M. C.; Yeung, M. C. L.; Yam, V. W. W. *Chem. Sci.* **2010**, *1*, 477−482.
(14) Tam, A. Y. Y.; Wong, K. M. C.; Zhu, N.; Wang, G. X.; Yam, V. W. W. *Langmuir* **2009**, *25*, 8685−8695.
(15) Tam, A. Y. Y.; Wong, K. M. C.; Yam, V. W. W. *Chem.—Eur. J.* **2009**, *15*, 4775−4778.
(16) Yu, C.; Chan, K. H. Y.; Wong, K. M. C.; Yam, V. W. W. *Chem.—Eur. J.* **2008**, *14*, 4577−4584.
(17) Yu, C.; Chan, K. H. Y.; Wong, K. M. C.; Yam, V. W. W. *Chem. Commun.* **2009**, 3756−3758.
(18) Yu, C.; Chan, K. H. Y.; Wong, K. M. C.; Yam, V. W. W. *Proc. Natl. Acad. Sci. U.S.A.* **2006**, *103*, 19652−19657.
(19) Yam, V. W. W.; Chan, K. H. Y.; Wong, K. M. C.; Chu, B. W. K. *Angew. Chem., Int. Ed.* **2006**, *45*, 6169−6173.
(20) Yeung, M. C. L.; Yam, V. W. W. *Chem.—Eur. J.* **2011**, *17*, 11987−11990.
(21) Yam, V. W. W.; Tang, R. P. L.; Wong, K. M. C.; Cheung, K. K. *Organometallics* **2001**, *20*, 4476−4482.
(22) Williams, J. A. G. *Top. Curr. Chem.* **2007**, *281*, 205−268.
(23) McGuire, R.; McGuire, M. C.; McMillin, D. R. *Coord. Chem. Rev.* **2010**, *254*, 2574−2583.
(24) Eryazici, I.; Moorefield, C. N.; Newkome, G. R. *Chem. Rev.* **2008**, *108*, 1834−1895.
(25) Wong, K. M. C.; Yam, V. W. W. *Coord. Chem. Rev.* **2007**, *251*, 2477−2488.
(26) Camerel, F.; Ziessel, R.; Donnio, B.; Bourgogne, C.; Guillon, D.; Schmutz, M.; Iacovita, C.; Bucher, J. P. *Angew. Chem., Int. Ed.* **2007**, *46*, 2659−2662.
(27) Ji, Z.; Azenkeng, A.; Hoffmann, M.; Sun, W. *Dalton Trans.* **2009**, 7725−7733.
(28) Muro, M. L.; Rachford, A. A.; Wang, X.; Castellano, F. N. *Top. Organomet. Chem.* **2010**, *29*, 159−191.
(29) Ji, Z.; Li, Y. J.; Sun, W. *Inorg. Chem.* **2008**, *47*, 7599−7607.
(30) Yang, Q. Z.; Wu, L. Z.; Wu, Z. X.; Zhang, L. P.; Tung, C. H. *Inorg. Chem.* **2002**, *41*, 5653−5655.
(31) Guo, F.; Sun, W.; Liu, Y.; Schanze, K. *Inorg. Chem.* **2005**, *44*, 4055−4065.
(32) Guo, F.; Sun, W. *J. Phys. Chem. B* **2006**, *110*, 15029−15036.
(33) Zhou, X.; Zhang, H. X.; Pan, Q. J.; Xia, B. H.; Tang, A. C. *J. Phys. Chem. A* **2005**, *109*, 8809−8818.
(34) Han, X.; Wu, L. Z.; Si, G.; Pan, J.; Yang, Q. Z.; Zhang, L. P.; Tung, C. H. *Chem.—Eur. J.* **2007**, *13*, 1231−1239.
(35) Wong, K. M. C.; Tang, W. S.; Chu, B. W. K.; Zhu, N.; Yam, V. W. W. *Organometallics* **2004**, *23*, 3459−3465.
(36) Rachford, A. A.; Goeb, S.; Ziessel, R.; Castellano, F. N. *Inorg. Chem.* **2008**, *47*, 4348−4355.
(37) Chakraborty, S.; Wadas, T. J.; Hester, H.; Flaschenreim, C.; Schmehl, R.; Eisenberg, R. *Inorg. Chem.* **2005**, *44*, 6284−6293.
(38) Chakraborty, S.; Wadas, T. J.; Hester, H.; Schmehl, R.; Eisenberg, R. *Inorg. Chem.* **2005**, *44*, 6865−6878.
(39) Yang, Y.; Zhang, D.; Wu, L. Z.; Chen, B.; Zhang, L. P.; Tung, C. H. *J. Org. Chem.* **2004**, *69*, 4788−4791.
(40) Zhang, D.; Wu, L. Z.; Yang, Q. Z.; Li, X. H.; Zhang, L. P.; Tung, C. H. *Org. Lett.* **2003**, *5*, 3221−3224.
(41) Zhang, D.; Wu, L. Z.; Zhou, L.; Han, X.; Yang, Q. Z.; Zhang, L. P.; Tung, C. H. *J. Am. Chem. Soc.* **2004**, *126*, 3440−3441.
(42) Du, P.; Knowles, K.; Eisenberg, R. *J. Am. Chem. Soc.* **2008**, *130*, 12576−12577.
(43) Du, P.; Schneider, J.; Jarosz, P.; Eisenberg, R. *J. Am. Chem. Soc.* **2006**, *128*, 7726−7727.
(44) Du, P.; Schneider, J.; Jarosz, P.; Zhang, J.; Brennessel, W. W.; Eisenberg, R. *J. Phys. Chem. B* **2007**, *111*, 6887−6894.
(45) Jarosz, P.; Du, P.; Schneider, J.; Lee, S. H.; McCamant, D.; Eisenberg, R. *Inorg. Chem.* **2009**, *48*, 9653−9663.
(46) Yang, Q. Z.; Tong, Q. X.; Wu, L. Z.; Wu, Z. X.; Zhang, L. P.; Tung, C. H. *Eur. J. Inorg. Chem.* **2004**, 1948−1954.

(47) Tang, W. S.; Lu, X. X.; Wong, K. M. C.; Yam, V. W. W. *J. Mater. Chem.* **2005**, *15*, 2714−2720.
(48) Fan, Y.; Zhu, Y. M.; Dai, F. R.; Zhang, L. Y.; Chen, Z. N. *Dalton Trans.* **2007**, 3885−3892.
(49) Lo, H. S.; Yip, S. K.; Wong, K. M. C.; Zhu, N.; Yam, V. W. W. *Organometallics* **2006**, *25*, 3537−3540.
(50) Wong, K. M. C.; Tang, W. S.; Lu, X. X.; Zhu, N.; Yam, V. W. W. *Inorg. Chem.* **2005**, *44*, 1492−1498.
(51) Fan, Y.; Zhang, L. Y.; Dai, F. R.; Shi, L. X.; Chen, Z. N. *Inorg. Chem.* **2008**, *47*, 2811−2819.
(52) Sun, W.; Wu, Z. X.; Yang, Q. Z.; Wu, L. Z.; Tung, C. H. *Appl. Phys. Lett.* **2003**, *82*, 850−852.
(53) Scarpaci, A.; Monnereau, C.; Hergue, N.; Blart, E.; Legoupy, S.; Odobel, F.; Gorfo, A.; Perez-Moreno, J.; Clays, K.; Asselberghs, I. *Dalton Trans.* **2009**, 4538−4546.
(54) Nastasi, F.; Puntoriero, F.; Campagna, S.; Olivier, J. H.; Ziessel, R. *Phys. Chem. Chem. Phys.* **2010**, *12*, 7392−7402.
(55) Ziessel, R.; Diring, S.; Retailleau, P. *Dalton Trans.* **2006**, 3285−3290.
(56) Ma, D. L.; Shum, T. Y. T.; Zhang, F.; Che, C. M.; Yang, M. *Chem. Commun.* **2005**, 4675−4677.
(57) Wang, X.; Goeb, S.; Ji, Z.; Castellano, F. N. *J. Phys. Chem. B* **2010**, *114*, 14440−14449.
(58) Shikhova, E.; Danilov, E. O.; Kinayyigit, S.; Pomestchenko, I. E.; Tregubov, A. D.; Camerel, F.; Retailleau, P.; Ziessel, R.; Castellano, F. N. *Inorg. Chem.* **2007**, *46*, 3038−3048.
(59) Castellano, F. N.; Pomestchenko, I. E.; Shikhova, E.; Hua, F.; Muro, M. L.; Rajapakse, N. *Coord. Chem. Rev.* **2006**, *250*, 1819−1828.
(60) Ni, J.; Zhang, L. Y.; Chen, Z. N. *J. Organomet. Chem.* **2009**, *694*, 339−345.
(61) Nastasi, F.; Puntoriero, F.; Campagna, S.; Diring, S.; Ziessel, R. *Phys. Chem. Chem. Phys.* **2008**, *10*, 3982−3986.
(62) Zhu, M. X.; Lu, W.; Zhu, N.; Che, C. M. *Chem.—Eur. J.* **2008**, *14*, 9736−9746.
(63) Yam, V. W. W.; Wong, K. M. C.; Zhu, N. *Angew. Chem., Int. Ed.* **2003**, *42*, 1400−1403.
(64) Muro, M. L.; Diring, S.; Wang, X.; Ziessel, R.; Castellano, F. N. *Inorg. Chem.* **2008**, *47*, 6796−6803.
(65) Jarosz, P.; Lotito, K.; Schneider, J.; Kumaresan, D.; Schmehl, R.; Eisenberg, R. *Inorg. Chem.* **2009**, *48*, 2420−2428.
(66) Chen, Z.; Wong, K. M. C.; Kwok, E. C. H.; Zhu, N.; Zu, Y.; Yam, V. W. W. *Inorg. Chem.* **2011**, *50*, 2125−2132.
(67) Kwok, E. C. H.; Chan, M. Y.; Wong, K. M. C.; Lam, W. H.; Yam, V. W. W. *Chem.—Eur. J.* **2010**, *16*, 12244−12254.
(68) Ziessel, R.; Diring, S. *Tetrahedron Lett.* **2006**, *47*, 4687−4692.
(69) Lam, S. C. F.; Yam, V. W. W.; Wong, K. M. C.; Cheng, E. C. C.; Zhu, N. *Organometallics* **2005**, *24*, 4298−4305.
(70) Liu, X. Y.; Han, X.; Zhang, L. P.; Tung, C. H.; Wu, L. Z. *Phys. Chem. Chem. Phys.* **2010**, *12*, 13026−13033.
(71) Narayana-Prabhu, R.; Schmehl, R. H. *Inorg. Chem.* **2006**, *45*, 4319−4321.
(72) Guerchais, V.; Fillaut, J. L. *Coord. Chem. Rev.* **2011**, *255*, 2448−2457.
(73) McMillin, D. R.; Moore, J. J. *Coord. Chem. Rev.* **2002**, *229*, 113−121.
(74) Michalec, J. F.; Bejune, S. A.; Cuttell, D. G.; Summerton, G. C.; Gertenbach, J. A.; Field, J. S.; Haines, R. J.; McMillin, D. R. *Inorg. Chem.* **2001**, *40*, 2193−2200.
(75) Crites, D. K.; Cunningham, C. T.; McMillin, D. R. *Inorg. Chim. Acta* **1998**, *273*, 346−353.
(76) Aldridge, T. K.; Stacy, E. M.; McMillin, D. R. *Inorg. Chem.* **1994**, *33*, 722−727.
(77) Danilov, E. O.; Pomestchenko, I. E.; Kinayyigit, S.; Gentili, P. L.; Hissler, M.; Ziessel, R.; Castellano, F. N. *J. Phys. Chem. A* **2005**, *109*, 2465−2471.
(78) Gunderson, V. L.; Krieg, E.; Vagnini, M. T.; Iron, M. A.; Rybtchinski, B.; Wasielewski, M. R. *J. Phys. Chem. B* **2011**, *115*, 7533−7540.
(79) Jimenez, A. J.; Grimm, B.; Gunderson, V. L.; Vagnini, M. T.; Calderon, S. K.; Rodriguez-Morgade, M. S.; Wasielewski, M. R.; Guldi, D. M.; Torres, T. *Chem.—Eur. J.* **2011**, *17*, 5024−5032.
(80) Prodi, A.; Chiorboli, C.; Scandola, F.; Iengo, E.; Alessio, E.; Dobrawa, R.; Wurthner, F. *J. Am. Chem. Soc.* **2005**, *127*, 1454−1462.
(81) Costa, R. D.; Cespedes-Guirao, F. J.; Bolink, H. J.; Fernandez-Lazaro, F.; Sastre-Santos, A.; Orti, E.; Gierschner, J. *J. Phys. Chem. C* **2009**, *113*, 19292−19297.
(82) Costa, R. D.; Cespedes-Guirao, F. J.; Orti, E.; Bolink, H. J.; Gierschner, J.; Fernandez-Lazaro, F.; Sastre-Santos, A. *Chem. Commun.* **2009**, 3886−3888.
(83) Vagnini, M. T.; Smeigh, A. L.; Blakemore, J. D.; Eaton, S. W.; Schley, N. D.; D'Souza, F.; Crabtree, R. H.; Brudvig, G. W.; Co, D. T.; Wasielewski, M. R. *Proc. Natl. Acad. Sci.*, [Online early access]. doi:10.1073/pnas.1202075109. Published ahead of print May 14, 2012.
(84) Castellano, F. N. *Dalton Trans.* **2012**, *41*, 8493−8501.
(85) Wurthner, F. *Chem. Commun.* **2004**, 1564−1579.
(86) Wasielewski, M. R. *J. Org. Chem.* **2006**, *71*, 5051−5066.
(87) Langhals, H. *Helv. Chim. Acta* **2005**, *88*, 1309−1343.
(88) Huang, C.; Barlow, S.; Marder, S. R. *J. Org. Chem.* **2011**, *76*, 2386−2407.
(89) Weil, T.; Vosch, T.; Hofkens, J.; Peneva, K.; Mullen, K. *Angew. Chem., Int. Ed.* **2010**, *49*, 9068−9093.
(90) Zhan, X.; Facchetti, A.; Barlow, S.; Marks, T. J.; Ratner, M. A.; Wasielewski, M. R.; Marder, S. R. *Adv. Mater.* **2011**, *23*, 268−284.
(91) Guo, F.; Ogawa, K.; Kim, Y. G.; Danilov, E. O.; Castellano, F. N.; Reynolds, J. R.; Schanze, K. S. *Phys. Chem. Chem. Phys.* **2007**, *9*, 2724−2734.
(92) Guo, F.; Kim, Y. G.; Reynolds, J. R.; Schanze, K. S. *Chem. Commun.* **2006**, 1887−1889.
(93) Weissman, H.; Shirman, E.; Ben-Moshe, T.; Cohen, R.; Leitus, G.; Shimon, L. J. W.; Rybtchinski, B. *Inorg. Chem.* **2007**, *46*, 4790−4792.
(94) Rachford, A. A.; Goeb, S.; Castellano, F. N. *J. Am. Chem. Soc.* **2008**, *130*, 2766−1767.
(95) Danilov, E. O.; Rachford, A. A.; Goeb, S.; Castellano, F. N. *J. Phys. Chem. A* **2009**, *113*, 5763−5768.
(96) Golubkov, G.; Weissman, H.; Shirman, E.; Wolf, S. G.; Pinkas, I.; Rybtchinski, B. *Angew. Chem., Int. Ed.* **2009**, *48*, 926−930.
(97) Gebers, J.; Rolland, D.; Frauenrath, H. *Angew. Chem., Int. Ed.* **2009**, *48*, 4480−4483.
(98) Tidhar, Y.; Weissman, H.; Wolf, S. G.; Gulino, A.; Rybtchinski, B. *Chem.—Eur. J.* **2011**, *17*, 6068−6075.
(99) Rajasingh, P.; Cohen, R.; Shirman, E.; Shimon, L. J. W.; Rybtchinski, B. *J. Org. Chem.* **2007**, *72*, 5973−5979.
(100) Price, J. H.; Williamson, A. N.; Schramm, R. F.; Wayland, B. B. *Inorg. Chem.* **1972**, *11*, 1280−1284.
(101) Yip, H. K.; Cheng, L. K.; Cheung, K. K.; Che, C. M. *J. Chem. Soc., Dalton Trans.* **1993**, 2933−2938.
(102) Yamazaki, S.; Deeming, A. J. *J. Chem. Soc., Dalton Trans.* **1993**, 3051−3057.
(103) Adams, C. J.; Fey, N.; Harrison, Z. A.; Sazanovich, I. V.; Towrie, M.; Weinstein, J. A. *Inorg. Chem.* **2008**, *47*, 8242−8257.
(104) Hua, F.; Kinayyigit, S.; Rachford, A. A.; Shikhova, E. A.; Goeb, S.; Cable, J. R.; Adams, C. J.; Kirschbaum, K.; Pinkerton, A. A.; Castellano, F. N. *Inorg. Chem.* **2007**, *46*, 8771−8783.
(105) Spano, F. C. *Acc. Chem. Res.* **2010**, *43*, 429−439.
(106) Abdel-Shafi, A. A.; Beer, P. D.; Mortimer, R. J.; Wilkinson, F. *Helv. Chim. Acta* **2001**, *84*, 2784−2795.
(107) Shibano, Y.; Umeyama, T.; Matano, Y.; Tkachenko, N. V.; Lemmetyinen, H.; Araki, Y.; Ito, O.; Imahori, H. *J. Phys. Chem. C* **2007**, *111*, 6133−6142.
(108) Shibano, Y.; Umeyama, T.; Matano, Y.; Tkachenko, N. V.; Lemmetyinen, H.; Imahori, H. *Org. Lett.* **2006**, *8*, 4425−4428.
(109) Chen, L. X.; Xiao, S.; Yu, L. *J. Phys. Chem. B* **2006**, *110*, 11730−11738.
(110) van der Boom, T.; Hayes, R. T.; Zhao, Y.; Bushard, P. J.; Weiss, E. A.; Wasielewski, M. R. *J. Am. Chem. Soc.* **2002**, *124*, 9582−9590.

(111) Ford, W. E.; Kamat, P. V. *J. Phys. Chem.* **1987**, *91*, 6373−6380.
(112) Omberg, K. M.; Smith, G. D.; Kavaliunas, D. A.; Chen, P. Y.; Treadway, J. A.; Schoonover, J. R.; Palmer, R. A.; Meyer, T. J. *Inorg. Chem.* **1999**, *38*, 951−956.
(113) Dattelbaum, D. M.; Omberg, K. M.; Hay, P. J.; Gebhart, N. L.; Martin, R. L.; Schoonover, J. R.; Meyer, T. J. *J. Phys. Chem. A* **2004**, *108*, 3527−3536.
(114) Polyansky, D. E.; Danilov, E. O.; Castellano, F. N. *Inorg. Chem.* **2006**, *45*, 2370−2372.
(115) Yarnell, J. E.; Deaton, J. C.; McCusker, C. E.; Castellano, F. N. *Inorg. Chem.* **2011**, *50*, 7820−7830.
(116) Schoonover, J. R.; Gordon, K. C.; Argazzi, R.; Woodruff, W. H.; Peterson, K. A.; Bignozzi, C. A.; Dyer, R. B.; Meyer, T. J. *J. Am. Chem. Soc.* **1993**, *115*, 10996−10997.
(117) Chen, P. Y.; Palmer, R. A.; Meyer, T. J. *J. Phys. Chem. A* **1998**, *102*, 3042−3047.
(118) Butler, J. M.; George, M. W.; Schoonover, J. R.; Dattelbaum, D. M.; Meyer, T. J. *Coord. Chem. Rev.* **2007**, *251*, 492−514.
(119) Probst, B.; Rodenberg, A.; Guttentag, M.; Hamm, P.; Alberto, R. *Inorg. Chem.* **2010**, *49*, 6453−6460.
(120) Sazanovich, I. V.; Alamiry, M. A. H.; Best, J.; Bennett, R. D.; Bouganov, O. V.; Davies, E. S.; Grivin, V. P.; Meijer, A. J. H. M.; Plyusnin, V. F.; Ronayne, K. L.; Shelton, A. H.; Tikhomirov, S. A.; Towrie, M.; Weinstein, J. A. *Inorg. Chem.* **2008**, *47*, 10432−10445.
(121) Liang, B. L.; Zhang, Y. X.; Wang, Y. F.; Xu, W.; Li, X. Y. *J. Mol. Struct.* **2009**, *917*, 133−141.
(122) Sun, H.; Frei, H. *J. Phys. Chem. B* **1997**, *101*, 205−209.
(123) Frisch, M. J.; Trucks, G. W.; Schlegel, H. B.; Scuseria, G. E.; Robb, M. A.; Cheeseman, J. R.; Scalmani, G.; Barone, V.; Mennucci, B.; Petersson, G. A.; Nakatsuji, H.; Caricato, M.; Li, X.; Hratchian, H. P.; Izmaylov, A. F.; Bloino, J.; Zheng, G.; Sonnenberg, J. L.; Hada, M.; Ehara, M.; Toyota, K.; Fukuda, R.; Hasegawa, J.; Ishida, M.; Nakajima, T.; Honda, Y.; Kitao, O.; Nakai, H.; Vreven, T.; Montgomery, Jr., J. A.; Peralta, J. E.; Ogliaro, F.; Bearpark, M.; Heyd, J. J.; Brothers, E.; Kudin, K. N.; Staroverov, V. N.; Kobayashi, R.; Normand, J.; Raghavachari, K.; Rendell, A.; Burant, J. C.; Iyengar, S. S.; Tomasi, J.; Cossi, M.; Rega, N.; Millam, J. M.; Klene, M.; Knox, J. E.; Cross, J. B.; Bakken, V.; Adamo, C.; Jaramillo, J.; Gomperts, R.; Stratmann, R. E.; Yazyev, O.; Austin, A. J.; Cammi, R.; Pomelli, C.; Ochterski, J. W.; Martin, R. L.; Morokuma, K.; Zakrzewski, V. G.; Voth, G. A.; Salvador, P.; Dannenberg, J. J.; Dapprich, S.; Daniels, A. D.; Farkas, O.; Foresman, J. B.; Ortiz, J. V.; Cioslowski, J.; Fox, D. J. *Gaussian 09*, revision A.01; Gaussian, Inc.: Wallingford, CT, 2009.